REPORT DOCUMENTATION PAGE

Form Approved
OMB No. 0704-0188

1. REPORT DATE *(DD-MM-YYYY)*	**2. REPORT TYPE**	**3. DATES COVERED** *(From - To)*
20 April 2012	Briefing Charts	20 April 2012 – 27 April 2012

4. TITLE AND SUBTITLE
CPU and GPU-based Numerical Simulations of Combustion Processes
(BRIEFING CHARTS)

5a. CONTRACT NUMBER

5b. GRANT NUMBER

5c. PROGRAM ELEMENT NUMBER

6. AUTHOR(S)
Le, H.; Cole, L.; Cambier, J.; and Karagozian, A.

5d. PROJECT NUMBER

5e. TASK NUMBER

5f. WORK UNIT NUMBER
23041057

7. PERFORMING ORGANIZATION NAME(S) AND ADDRESS(ES)
Air Force Research Laboratory (AFMC)
AFRL/RZSS
1 Ara Drive
Edwards AFB CA 93524-7013

8. PERFORMING ORGANIZATION REPORT NO.

9. SPONSORING / MONITORING AGENCY NAME(S) AND ADDRESS(ES)
Air Force Research Laboratory (AFMC)
AFRL/RQR
5 Pollux Drive
Edwards AFB CA 93524-7048

10. SPONSOR/MONITOR'S ACRONYM(S)

11. SPONSOR/MONITOR'S REPORT NUMBER(S)
AFRL-RZ-ED-VG-2012-105

12. DISTRIBUTION / AVAILABILITY STATEMENT
Distribution A: Approved for public release; distribution unlimited PA# 12246

13. SUPPLEMENTARY NOTES
For presentation at UCLA MAE Research & Technology Review Conference, Los Angeles, CA on 27 April 2012

14. ABSTRACT
CPU and GPU-based Numerical Simulations of Combustion Processes.

15. SUBJECT TERMS

16. SECURITY CLASSIFICATION OF:			**17. LIMITATION OF ABSTRACT**	**18. NUMBER OF PAGES**	**19a. NAME OF RESPONSIBLE PERSON**
a. REPORT	**b. ABSTRACT**	**c. THIS PAGE**			Jean-Luc Cambier
Unclassified	**Unclassified**	**Unclassified**	SAR	14	**19b. TELEPHONE NO** *(include area code)* NA

Standard Form 298 (Rev. 8-98)
Prescribed by ANSI Std. 239.18

UCLA MAE Research and Technology Review
April 27, 2012

CPU and GPU-based Numerical Simulations of Combustion Processes

Hai Le[1], Lord Cole[1], Jean-Luc Cambier[2], Ann Karagozian[1]

[1]University of California, Los Angeles

[2]Air Force Research Laboratory, Edwards AFB

Magnetohydrodynamic Augmentation of the Pulse Detonation Rocket Engines

- Pulse Detonation Rocket-Induced MHD Ejector (PDRIME)
  - Energy extract from exhaust flow by MHD generator
  - Seeded air stream acceleration by MHD accelerator for thrust enhancement and control

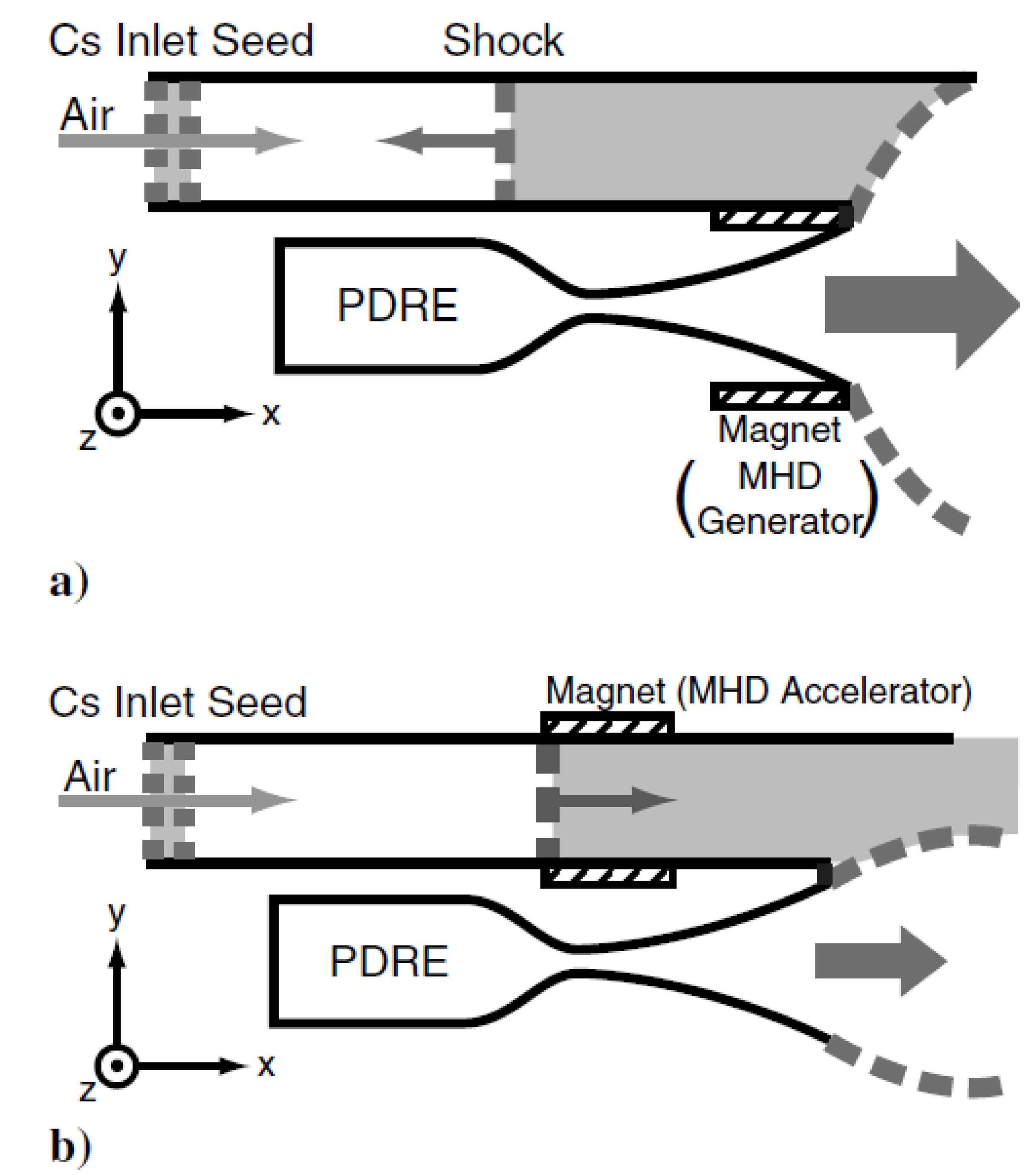

- Alternative concept: Magnetic piston
  - During PDE blowdown process, MHD extracts energy and applies to chamber gas via a magnetic piston or MHD generator to maintain constant chamber pressure and temperature

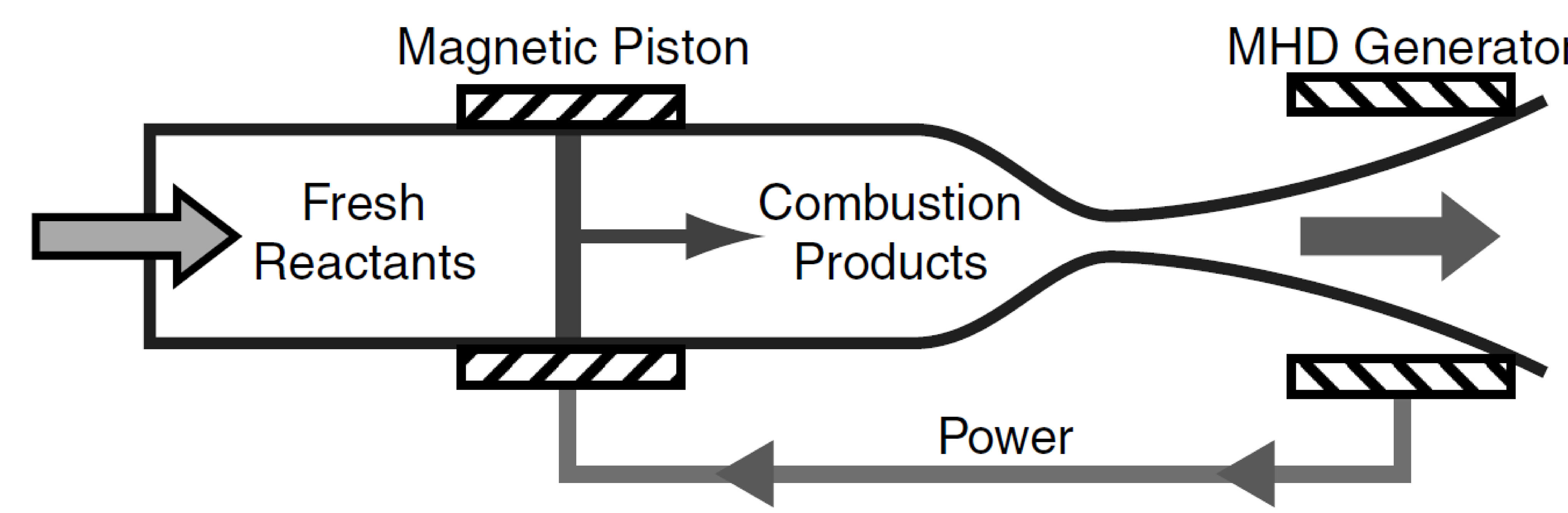

Simplified Physical Models

- Euler fluid transport with WENO

$$\mathbf{U_t + F(U)_x + G(U)_y = S(U) + M(U)}$$

- One-step kinetics (ionization of cesium)

$$\mathbf{Cs + e^- + M = Cs^+ + M}$$

$$\begin{pmatrix} \dot{\Omega}_{Cs} \\ \dot{\Omega}_{Cs^+} \end{pmatrix} = \frac{\mathrm{d}}{\mathrm{d}t} \begin{pmatrix} [Cs] \\ [Cs^+] \end{pmatrix} = \begin{pmatrix} -k_f[Cs][M] + k_r[Cs^+][M][e^-] \\ k_f[Cs][M] - k_r[Cs^+][M][e^-] \end{pmatrix}$$

- Fixed electromagnetic field line
  - Lorentz force

$$\mathbf{F}_L = \mathbf{J} \times \mathbf{B}$$

$$\mathbf{J} = \sigma(\mathbf{E} + \mathbf{u} \times \mathbf{B})$$

  - MHD energy source term

$$\mathbf{J} \cdot \mathbf{E} = \frac{\mathbf{J}^2}{\sigma} + \mathbf{u} \cdot (\mathbf{J} \times \mathbf{B})$$

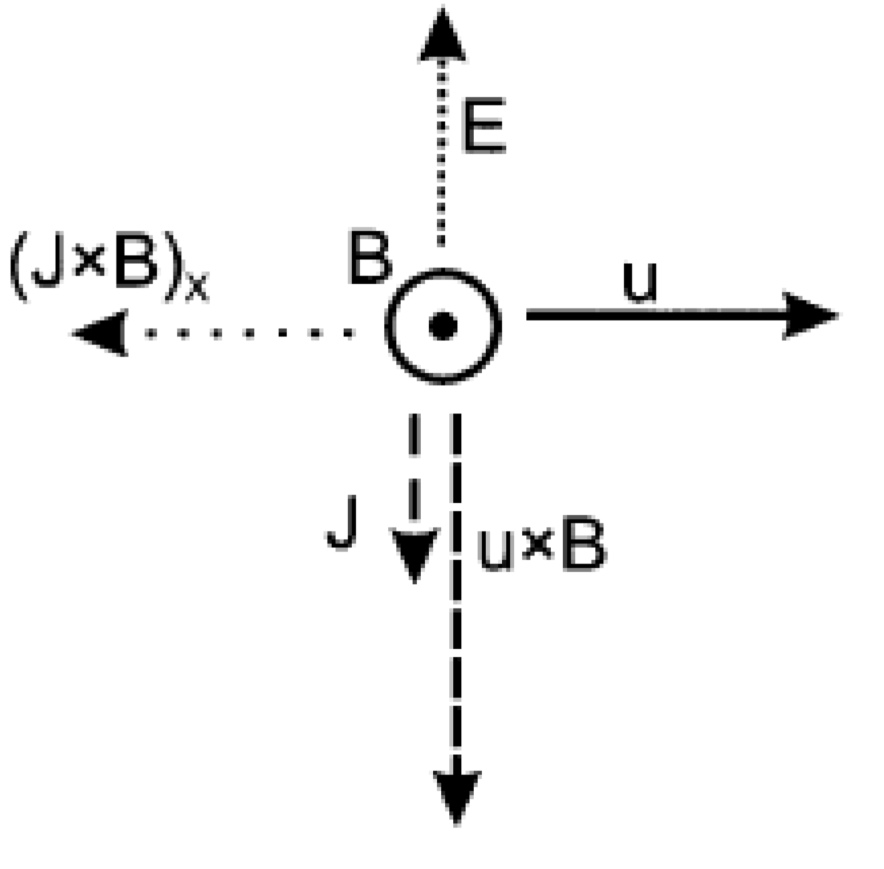

MHD Generator (Nozzle)

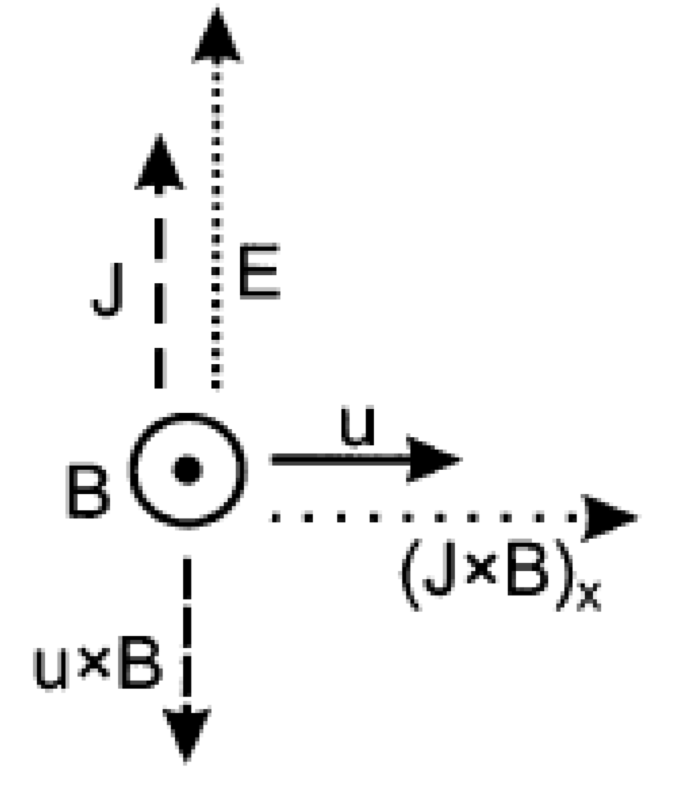

MHD Accelerator (Bypass tube)

Numerical Simulations of PDRIME

- Temperature contour of a PDRIME operating at 25 km, chamber temperature of 3000K and flight Mach number of 9
- Total impulse per cycle at 30 km and bypass area per unit length. Initial chamber of 3000 K and bypass length is 6 m. The chamber is seeded with 0.5% Cs and the bypass tube is seeded with 0.1% Cs (by moles).

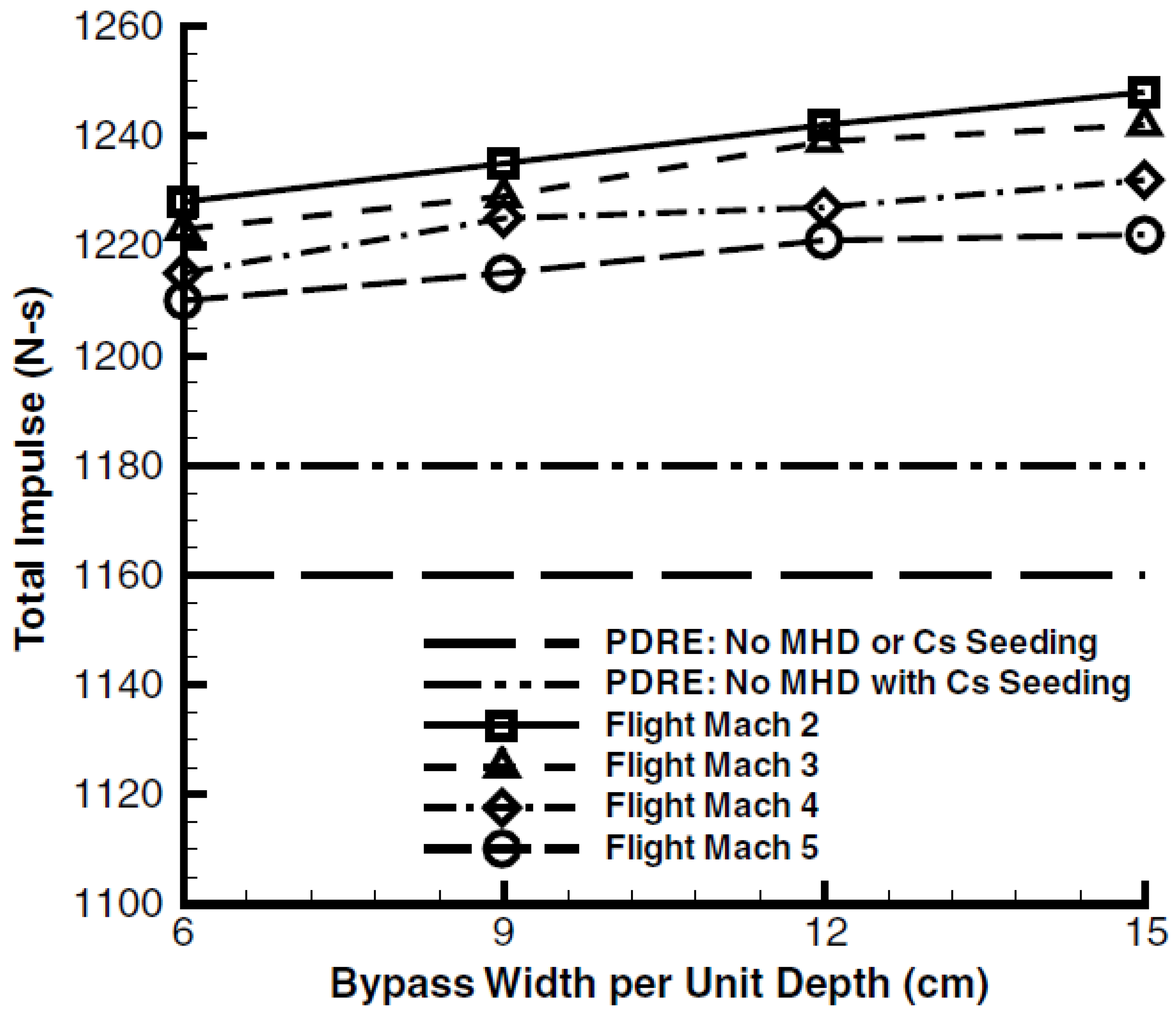

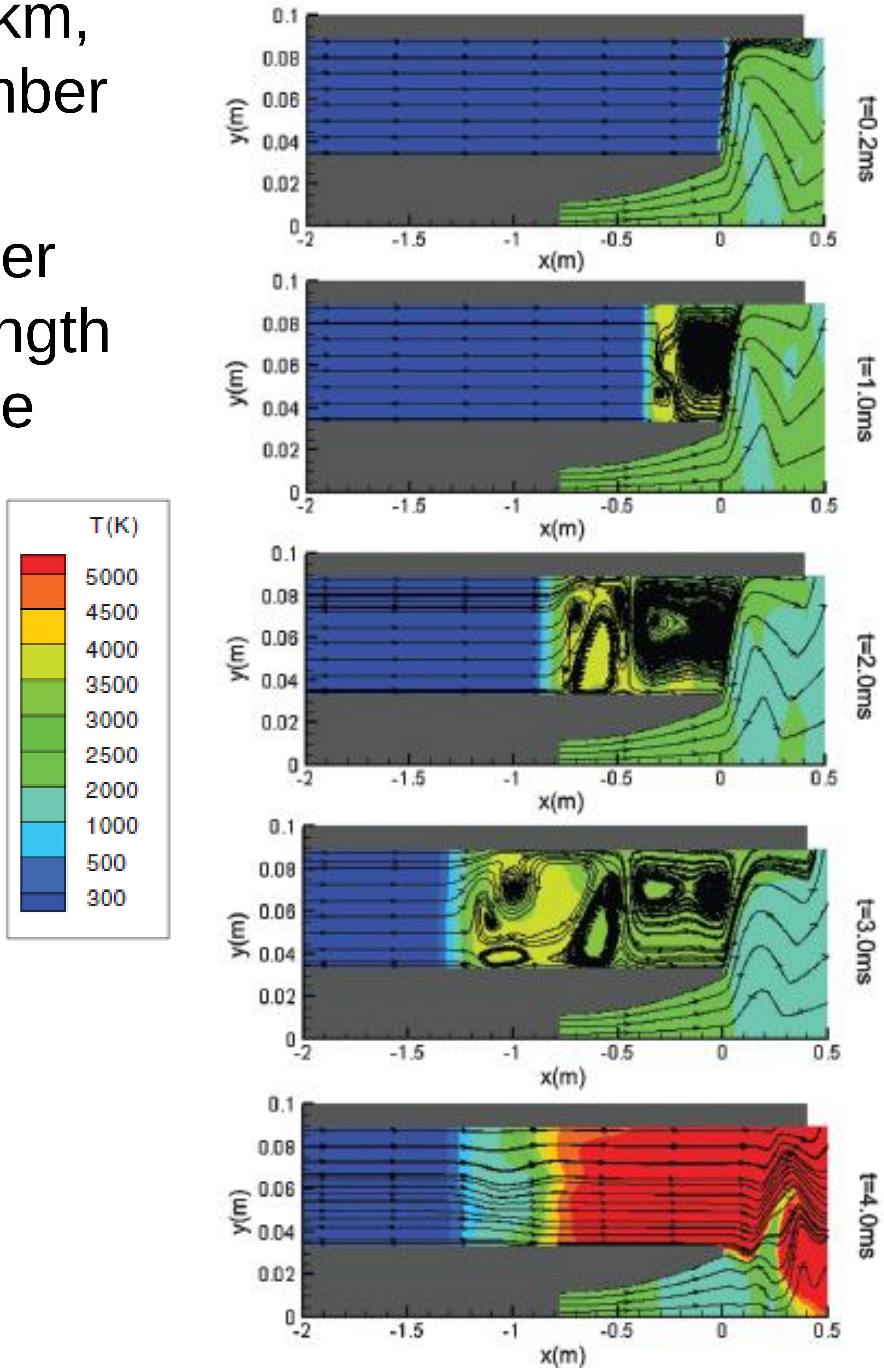

Detailed Physical Models

- Euler fluid transport with high-order shock capturing schemes: MP5, WENO, etc. in thermochemical nonequilibrium (2T model).
- Complex chemical kinetics for combustion processes
- Collisional-Radiative kinetics for electronic excitation and ionization.
- Electromagnetic field coupling via ideal and resistive MHD

$$\frac{dQ}{dt} + \frac{1}{V}\oint_S F_n dS = \dot{\Omega},$$

$$Q = \begin{pmatrix} \rho_1 \\ \vdots \\ \rho_n \\ \rho u \\ \rho v \\ \rho w \\ B_x \\ B_y \\ B_z \\ E \\ \rho \hat{s}_e \end{pmatrix}, \quad F_n = \begin{pmatrix} \rho_1 v_n \\ \vdots \\ \rho_n v_n \\ \rho u v_n + n_x p_\circ - B_x B_n/\mu_\circ \\ \rho v v_n + n_y p_\circ - B_y B_n/\mu_\circ \\ \rho w v_n + n_z p_\circ - B_z B_n/\mu_\circ \\ v_n B_x - u B_n \\ v_n B_y - v B_n \\ v_n B_z - w B_n \\ v_n(E + p_\circ) - B_n(\vec{v}\cdot\vec{B})/\mu_\circ \\ v_n S_e \end{pmatrix} \quad A = \frac{\partial F}{\partial Q} = \left(\begin{array}{ccccccccccc} u(1-y_1) & \dots & -uy_1 & y_1 & 0 & 0 & 0 & 0 & 0 & 0 & 0 \\ \vdots & \ddots & \vdots & \vdots & \vdots & \vdots & \vdots & \vdots & \vdots & \vdots & \vdots \\ -uy_n & \dots & u(1-y_n) & y_n & 0 & 0 & 0 & 0 & 0 & 0 & 0 \\ P_{\rho_1} - u^2 & \dots & P_{\rho_n} - u^2 & P_{m_x} + 2u & P_{m_y} & P_{m_z} & P_{B_x} - \frac{B_x}{\mu_\circ} & P_{B_y} + \frac{B_y}{\mu_\circ} & P_{B_z} + \frac{B_z}{\mu_\circ} & P_E & P_{S_e} \\ -uv & \dots & -uv & v & u & 0 & -\frac{B_y}{\mu_\circ} & -\frac{B_z}{\mu_\circ} & 0 & 0 & 0 \\ -uw & \dots & -uw & w & 0 & u & -\frac{B_z}{\mu_\circ} & 0 & -\frac{B_z}{\mu_\circ} & 0 & 0 \\ \frac{vB_x - uB_y}{\rho} & \dots & \frac{vB_x - uB_y}{\rho} & \frac{B_y}{\rho} & -\frac{B_x}{\rho} & 0 & -v & u & 0 & 0 & 0 \\ \frac{wB_z - uB_z}{\rho} & \dots & \frac{wB_z - uB_z}{\rho} & \frac{B_z}{\rho} & 0 & -\frac{B_z}{\rho} & -w & 0 & u & 0 & 0 \\ & & & & \multicolumn{3}{c}{\longleftarrow \partial f_E/\partial Q \longrightarrow} & & & & \\ -\frac{u}{\rho}S_e & \dots & -\frac{u}{\rho}S_e & \frac{1}{\rho}S_e & 0 & 0 & 0 & 0 & 0 & 0 & u \end{array}\right)$$

HPC Capability: Graphic Processing Units

- Graphic Processing Units
  - Graphic processing units containing a massive amount of processing cores designed for graphic rendering
  - GPU is faster than CPU on SIMD execution model.
  - GPGPU programing is very identical to traditional C/C++ (or Fortran). Object-Oriented features are available in CUDA.
  - GPU is much cheaper than CPU. The performance/dollar ratio for GPU is at least 16 times higher than CPU.

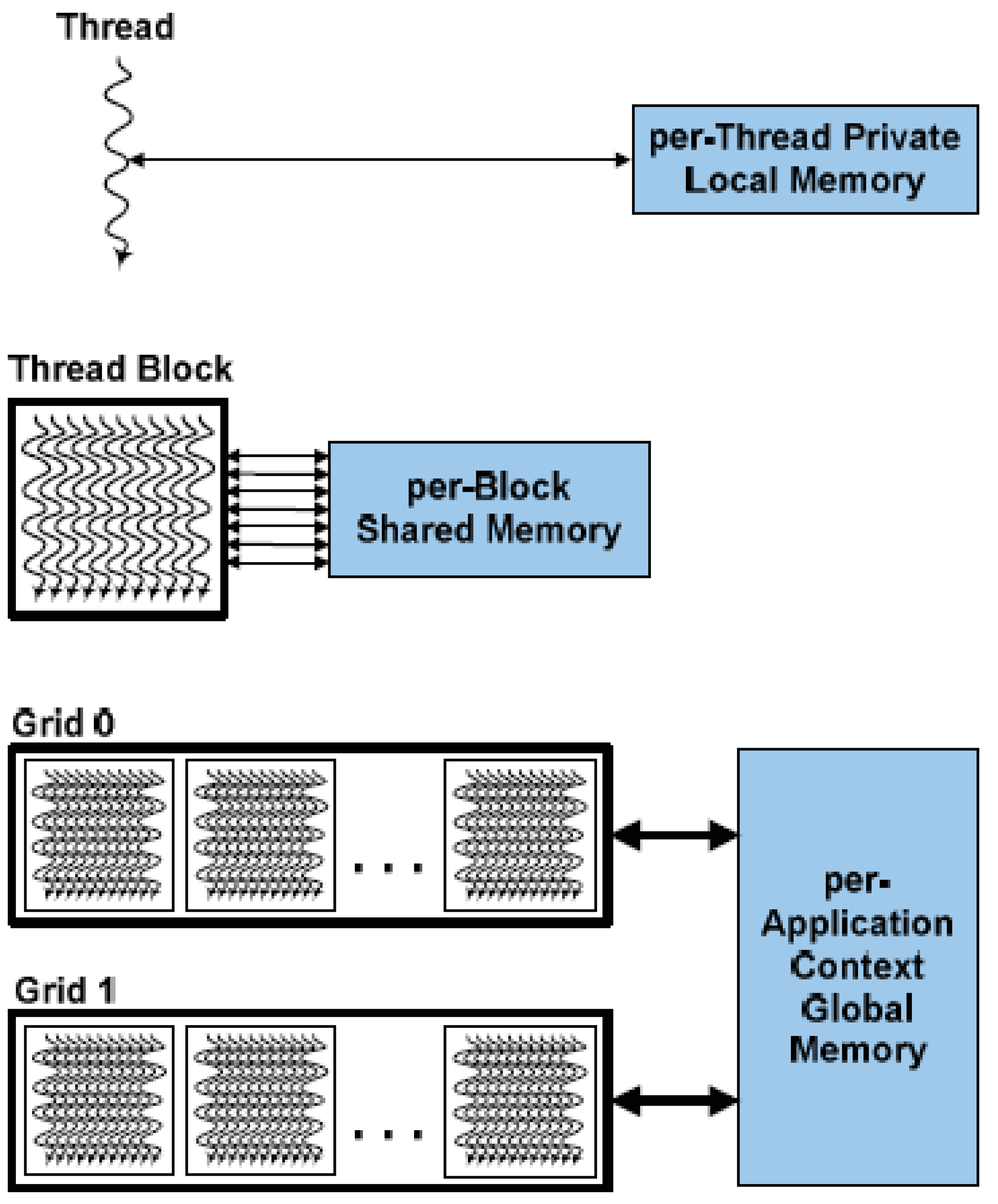

- Hoffman 2 ARK gpu queue configuration
  - 6 computing nodes (3 Tesla Fermi M2070 GPUs/node)
  - Supports MPI, CUDA, OpenCL, etc.

High-order Simulations of Fluid Flows

- Standard test cases for ideal gas flow:

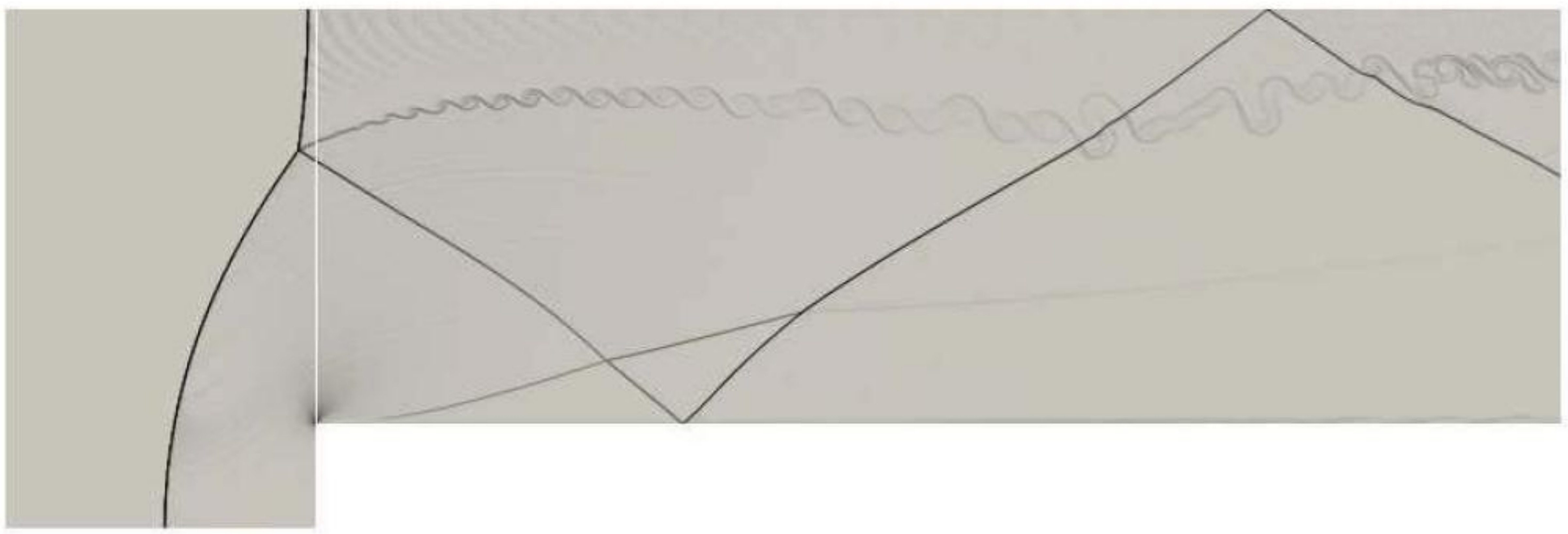

Forward step problem (800,000 cells)

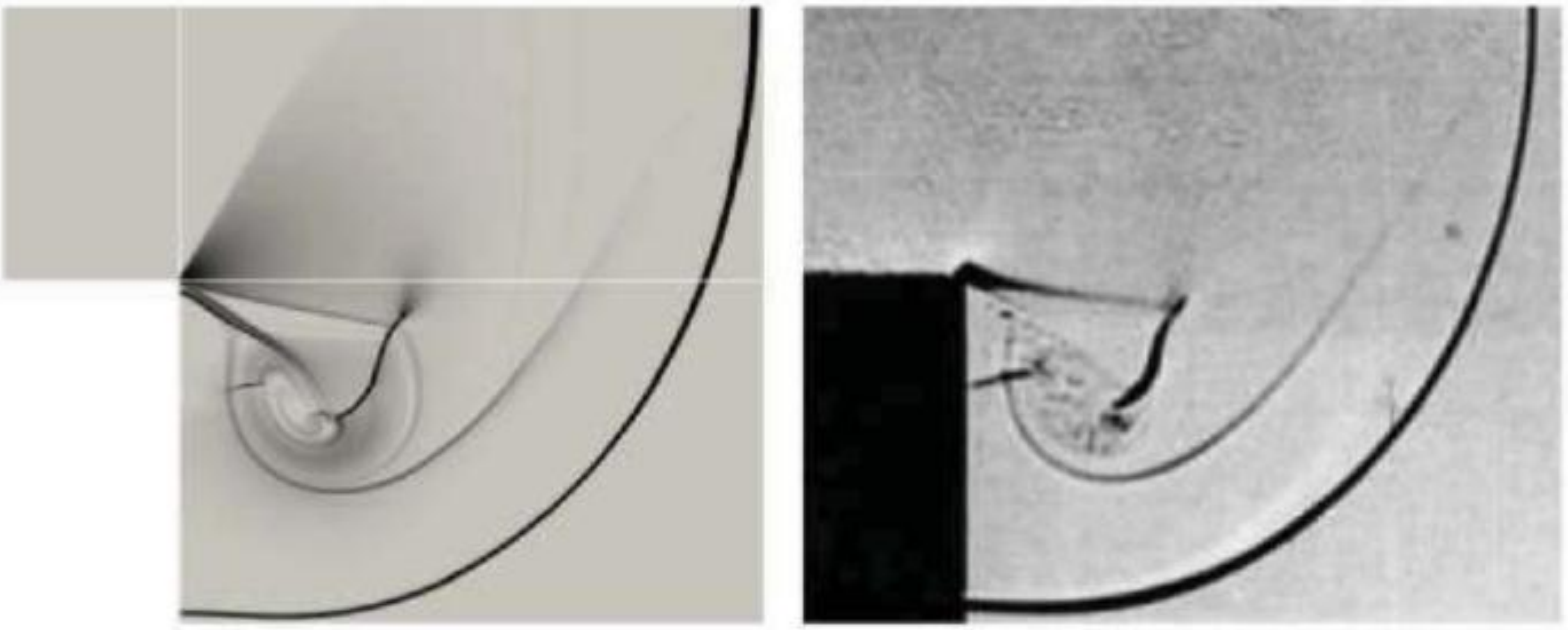

Backward step problem (27,000 cells)

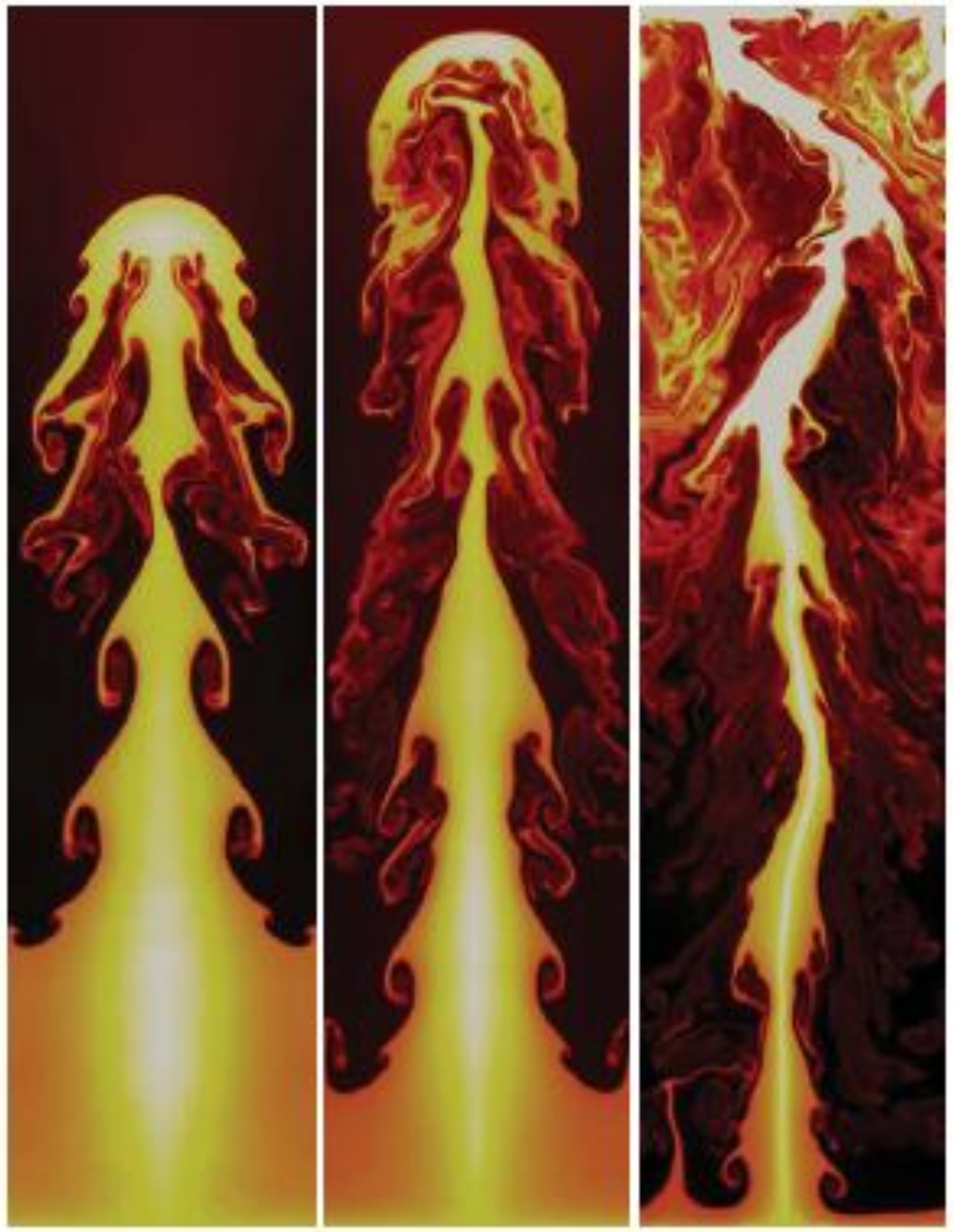

Rayleigh-Taylor instabilities problem (1.6 Mcells)

Complex Kinetics

- Chemical kinetics

$$\sum_s \nu'_{rs}[X_s] \rightleftarrows \sum_s \nu''_{rs}[X_s]$$

$$\dot{\omega}_s = \sum_r \nu_{rs} K_{fr} \prod_s [X_s]^{\nu'_{rs}} - \sum_r \nu_{rs} K_{br} \prod_s [X_s]^{\nu''_{rs}}$$

$$\nu_{rs} = \nu''_{rs} - \nu'_{rs}$$

- Collisional-Radiative (CR) Kinetics

$$\frac{dn_k}{dt} = \sum_{j<k}\{C^{ex}_{kj} n_e n_j - C^{ed}_{jk} n_e n_k - R_{jk}\} + \sum_h \sum_{j>k}\{C^{ed}_{kj} n_e n_j - C^{ex}_{jk} n_e n_k + R_{kj}\}$$
$$\sum_{j<k}\{C^{hx}_{kj} n_h n_j - C^{hd}_{jk} n_h n_k\} + \sum_h \sum_{j>k}\{C^{hd}_{kj} n_h n_j - C^{hx}_{jk} n_h n_k\}$$
$$-C^{ei}_k n_e n_k + C^{er}_k n_e^2 n_i - \sum_h C^{hi}_k n_h n_k + \sum_h C^{hr}_k n_e n_h n_i + R_k n_e n_i$$

- Implicit kinetics solver

$$\frac{d\mathbf{Q}^n}{dt} = \dot{\mathbf{\Omega}}^{n+1} \rightarrow \left(I - \Delta t \frac{\partial \dot{\mathbf{\Omega}}}{\partial \mathbf{Q}}\right) \frac{d\mathbf{Q}^n}{dt} = \dot{\mathbf{\Omega}}^n$$

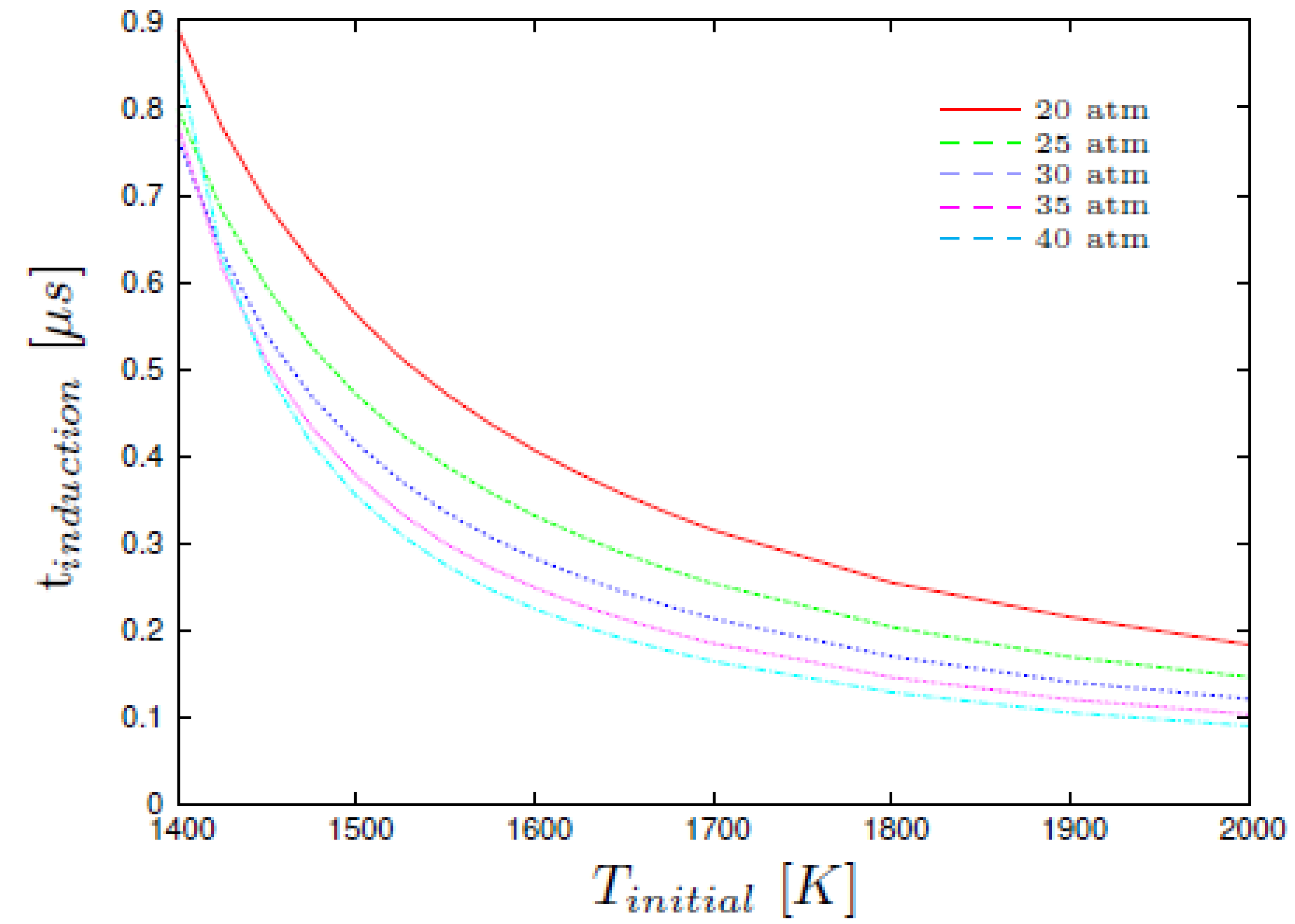

Induction delay time for Air mixture at various pressure and temperature

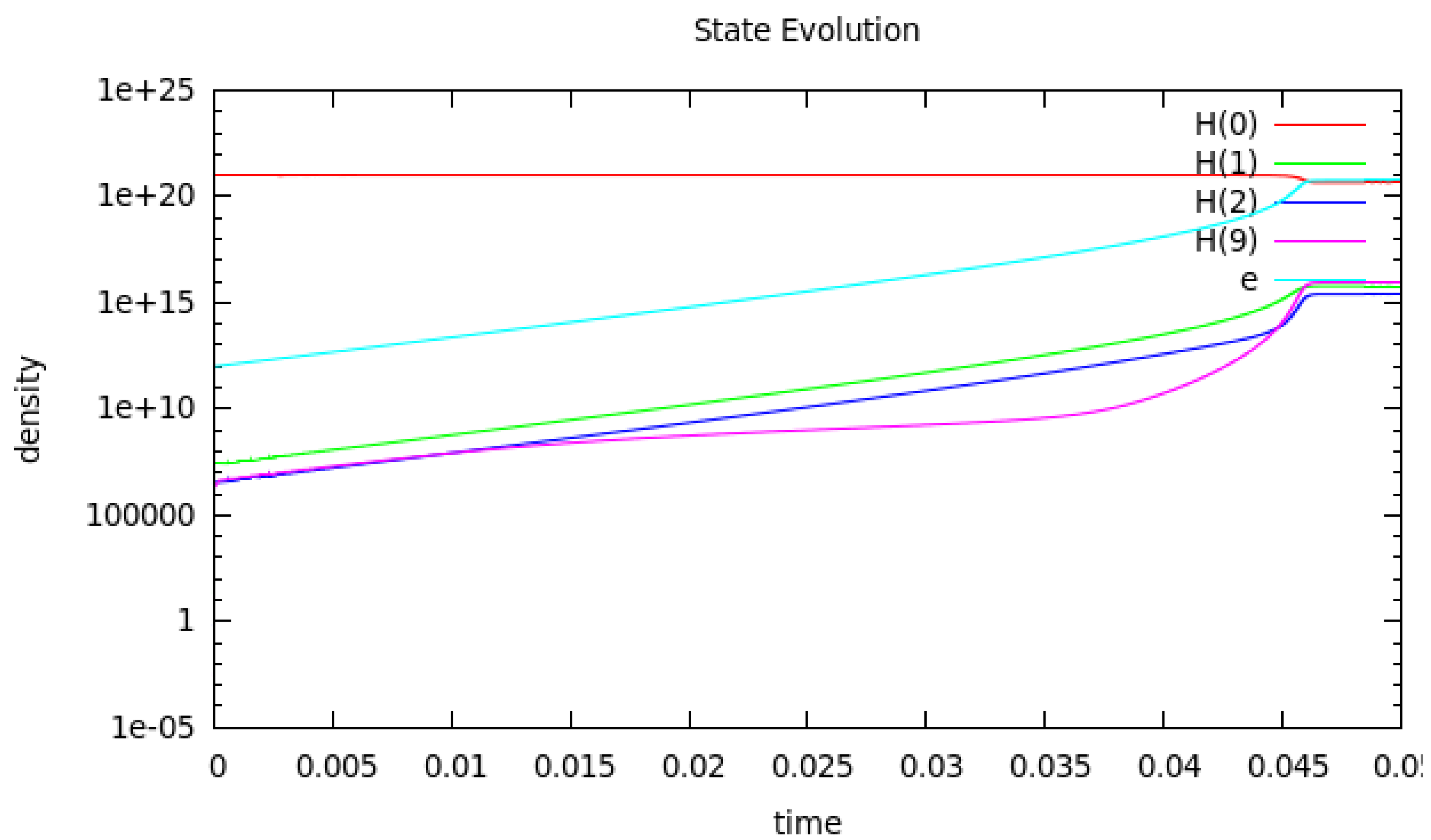

CR kinetics of electronic states of atomic hydrogen during isothermal heating process

Magnetohydrodynamic Simulations

- Ideal MHD test cases

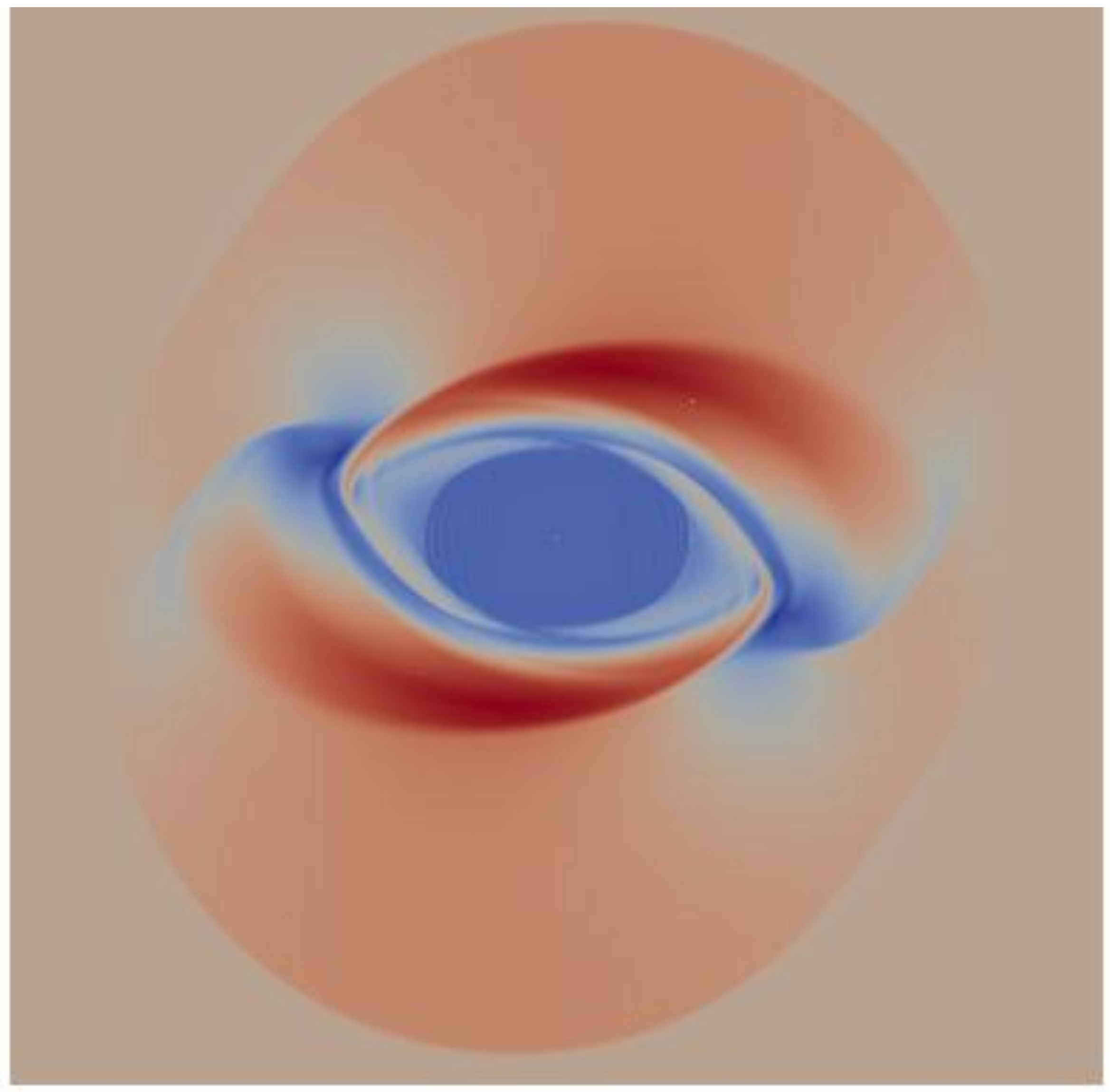

Rotor problem
(16,000 cells)

Orszag-Tang problem
(16,000 cells)

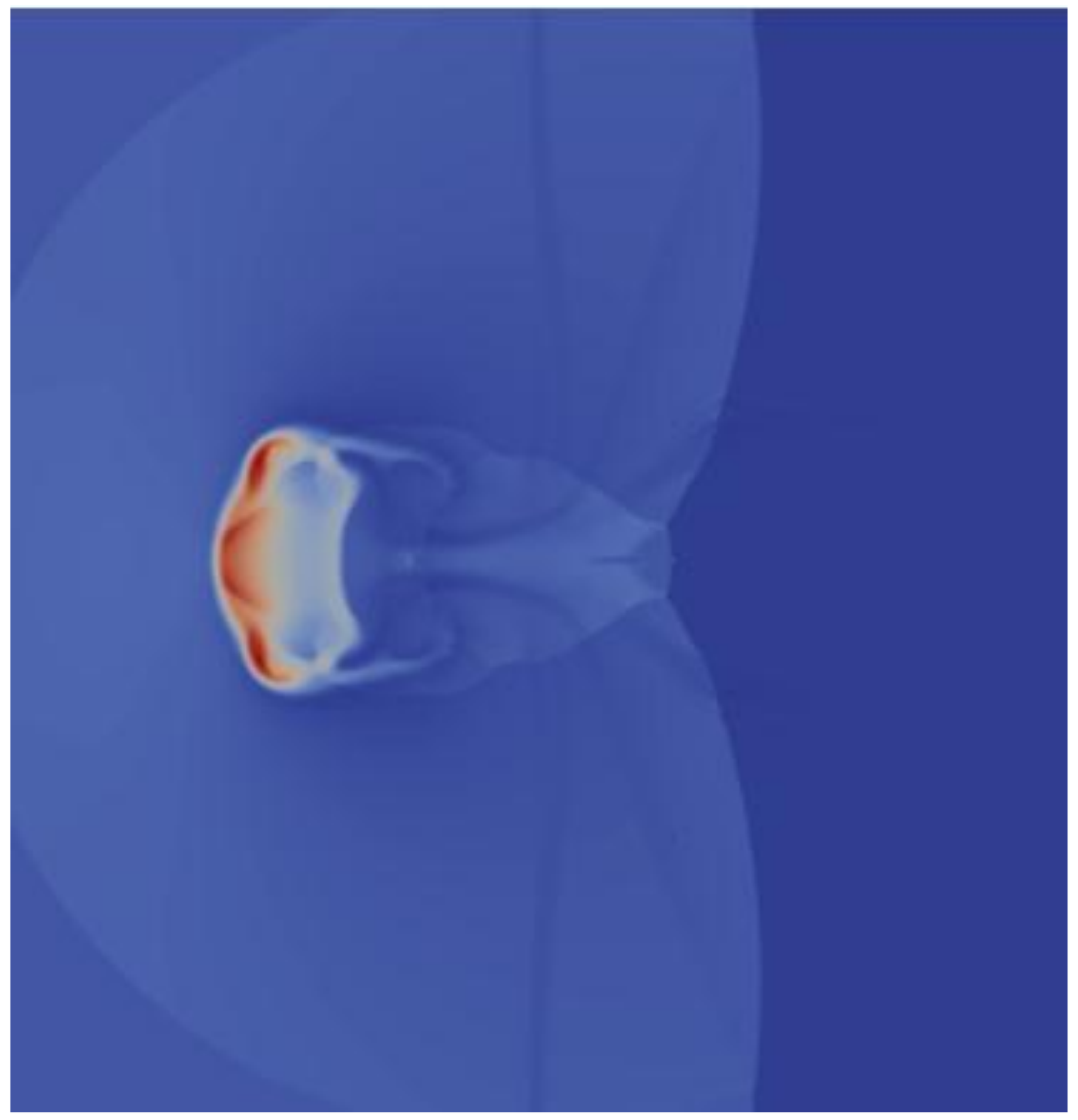

MHD cloud shock
(23,000 cells)

- Resistive MHD

$$\frac{\partial B^{\alpha}}{\partial t} + \nabla_{\beta}\left[u^{\beta} B^{\alpha} - u^{\alpha} B^{\beta}\right] = \nabla_{\beta}\left[\frac{1}{\sigma\mu_{0}}\left(\nabla^{\beta} B^{\alpha} - \nabla^{\alpha} B^{\beta}\right)\right]$$

$$\frac{\partial}{\partial t}\left[E_P + E_M\right] + \nabla_{\beta}\left[u^{\beta}\left(E_P + E_M\right) + u^{\alpha}\left(\overline{\overline{P}}^{\alpha\beta} + T_M^{\alpha\beta}\right)\right] = \nabla_{\alpha}\left[\frac{1}{\sigma\mu_o}\nabla_{\beta} T_M^{\alpha\beta}\right]$$

$$T_M^{\alpha\beta} = \frac{\vec{B}^2}{2\mu_o}\delta_{\alpha\beta} - \frac{B_\alpha B_\beta}{\mu_o}$$

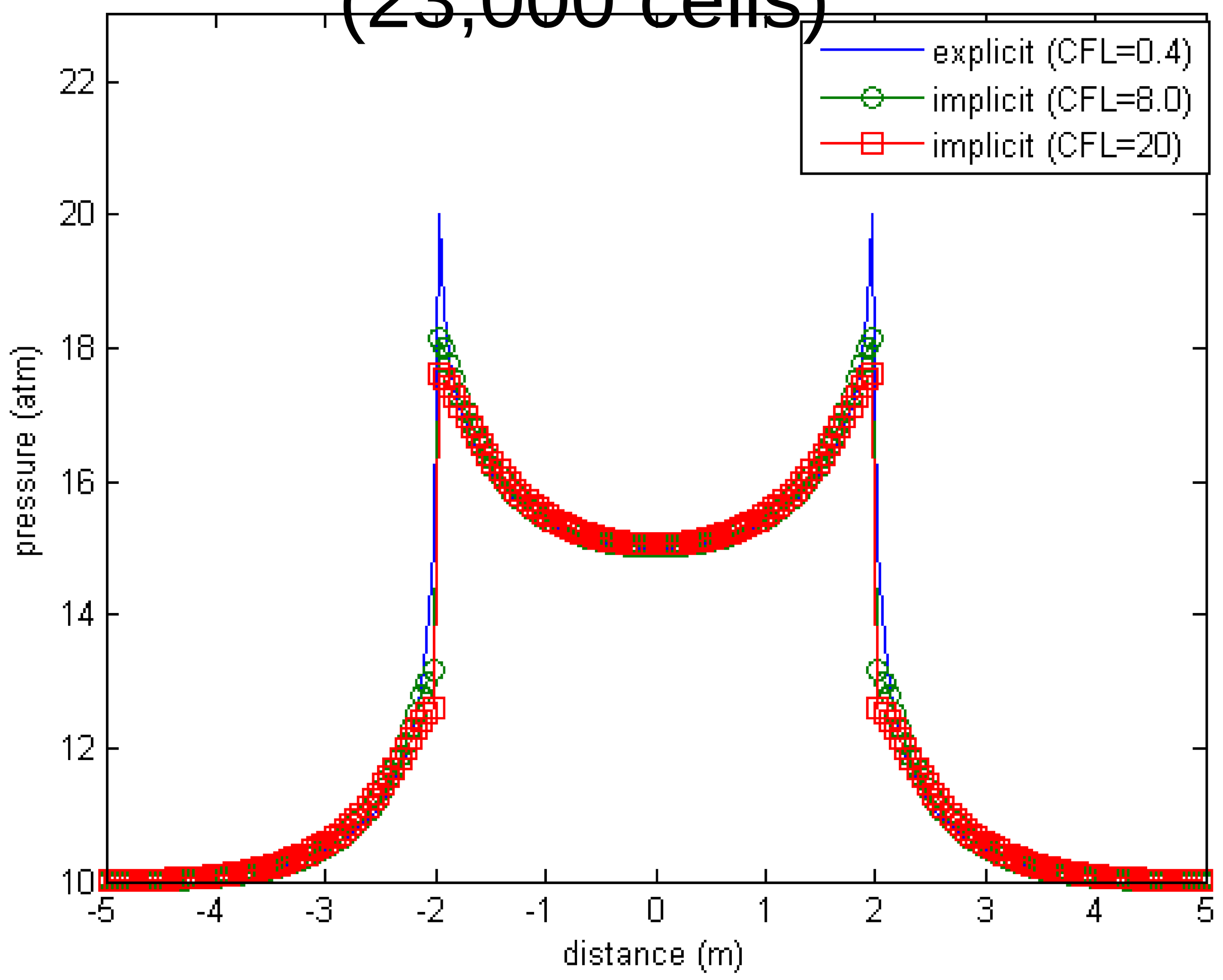

Comparison of heating rates (pressure rise) for explicit and implicit magnetic diffusion schemes

Flame-Shock Coupling: 1-D Dynamics of Instabilities

- Oscillatory patterns and distinct instability modes of a 1-D detonation wave at the CJ limit can be observed via high-order numerical simulation.
  - High frequency mode appears first and marks the transition from a stable CJ detonation
  - High amplitude (low frequency) mode appears later which directly couples the flame speed with the shock

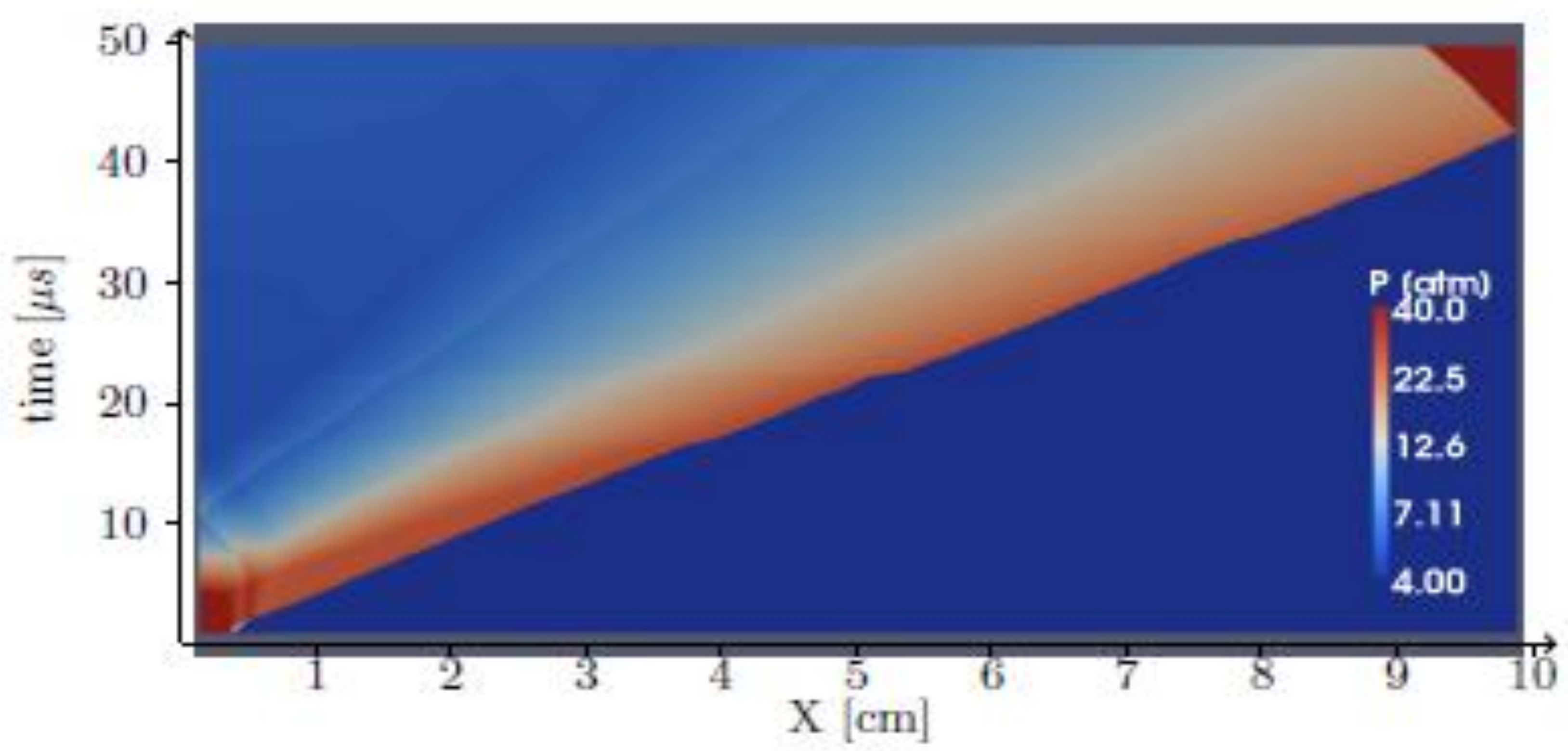

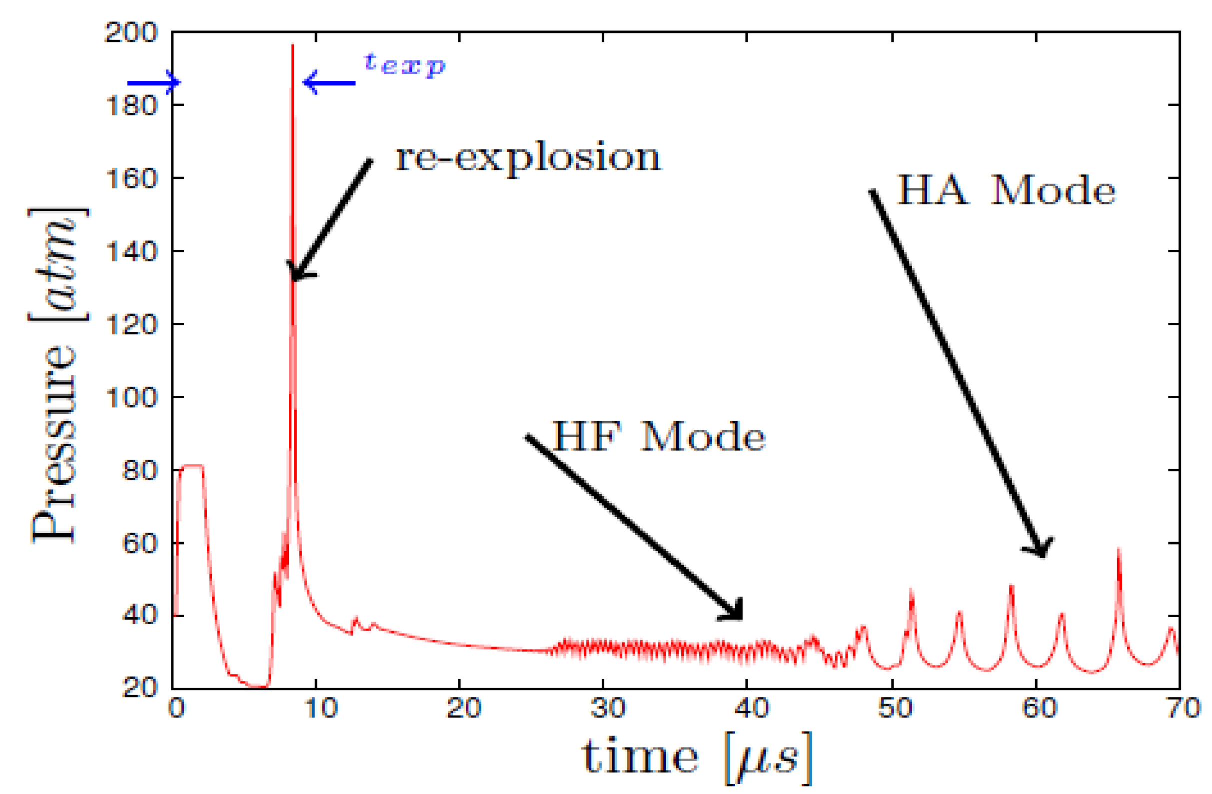

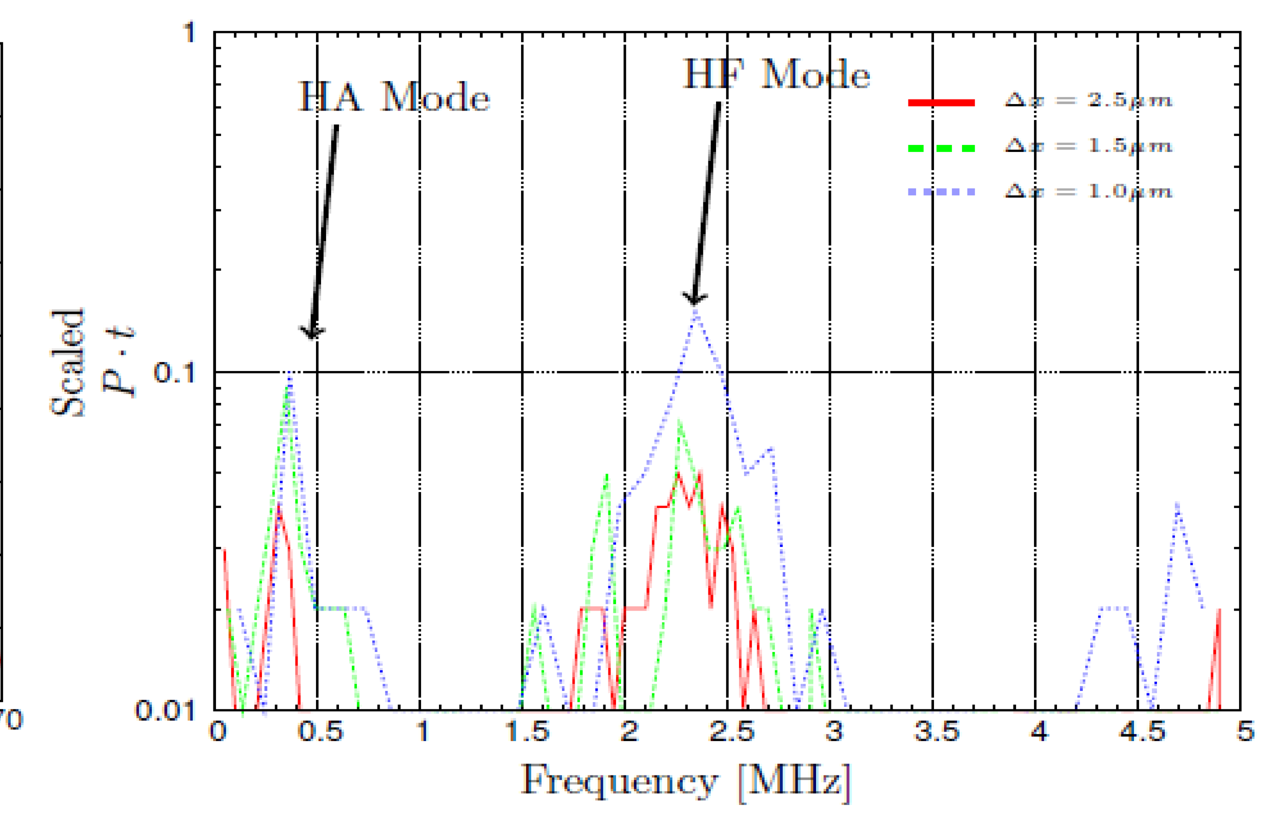

- The dynamics of a detonation wave can be explained by the strong coupling between fluid convection and kinetics.
  - Simple model: entropy and acoustic waves cycles in flame-shock coupling

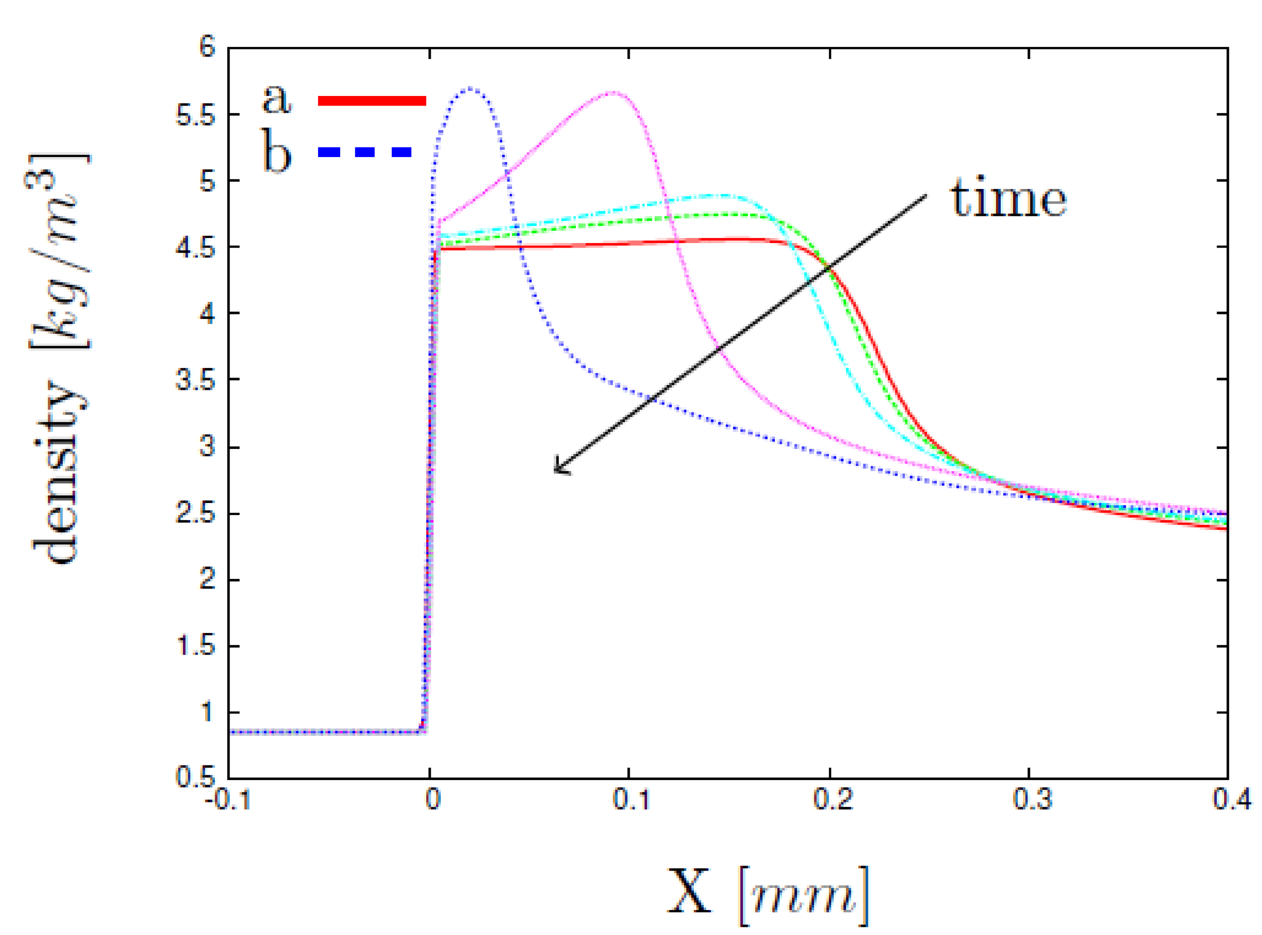

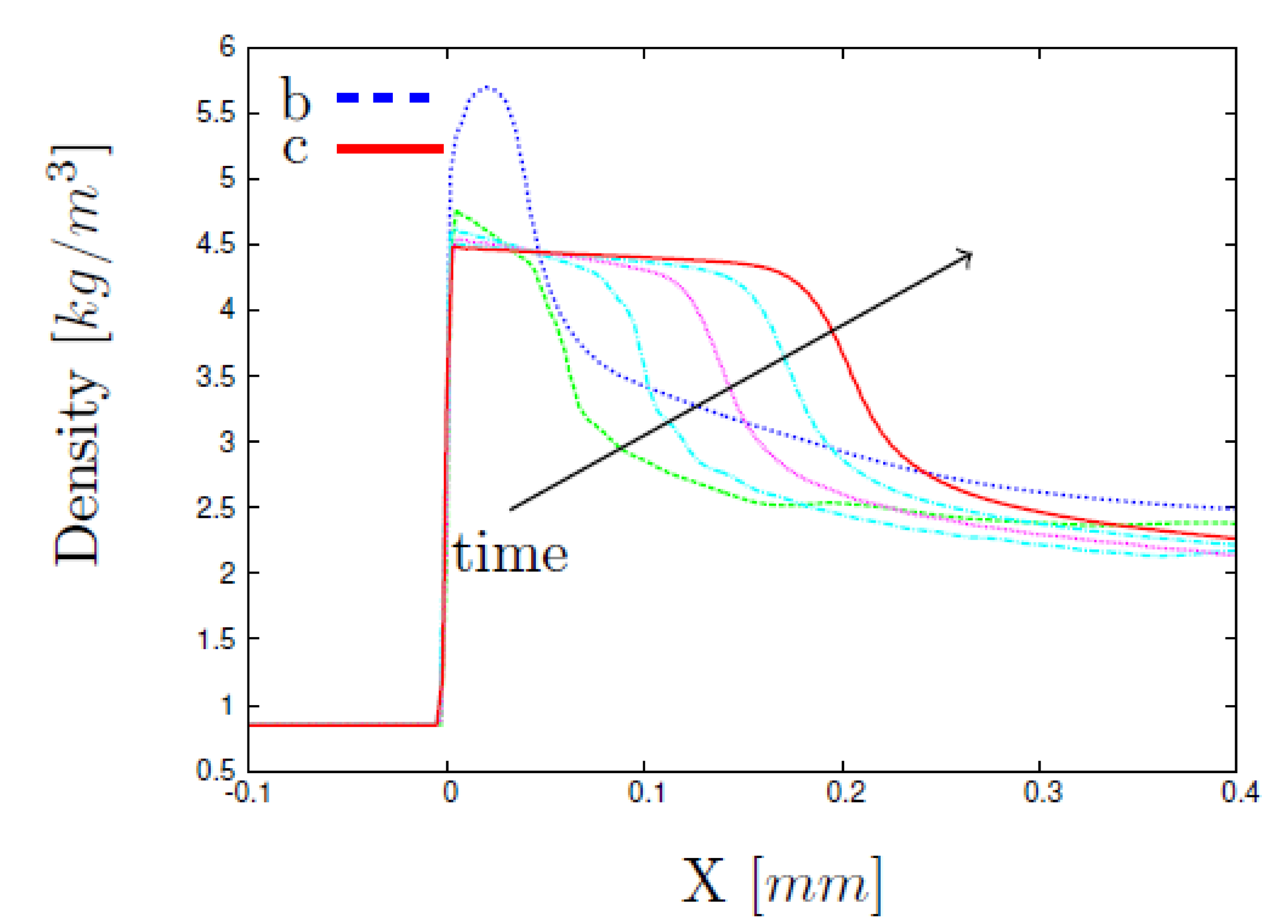

Flame-shock Coupling: Multi-dimensional Effects

- Influence of traverse waves
  - Unstable shock front due to interaction with the traverse waves.
  - The intersection of the lead shock and the traverse waves produces two triple points connected by a Mach stem that grows in width

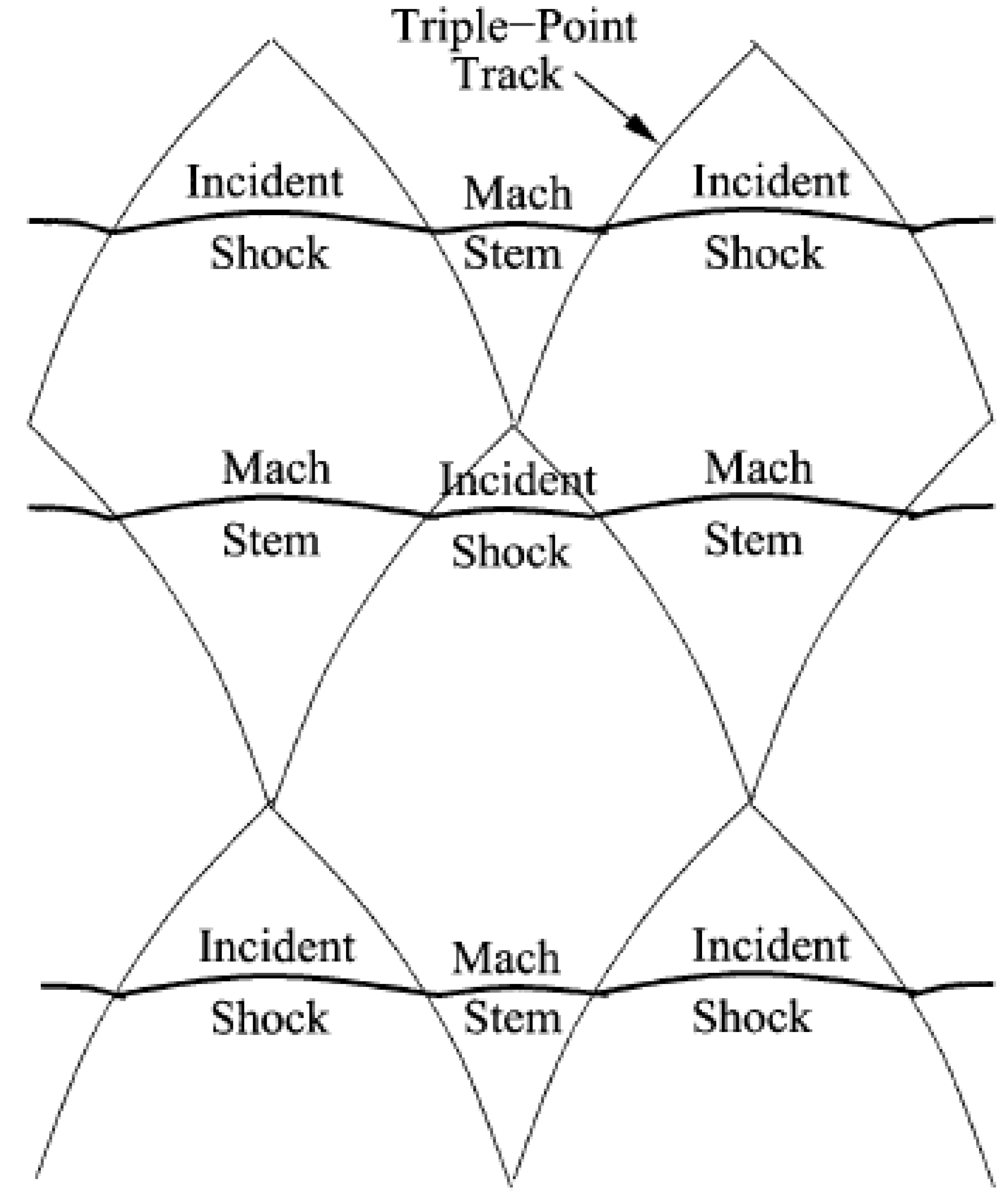

- Cellular pattern for 2D detonation simulation with complex kinetics
  - Characterize a network of triple points that are connected to smooth shock fronts

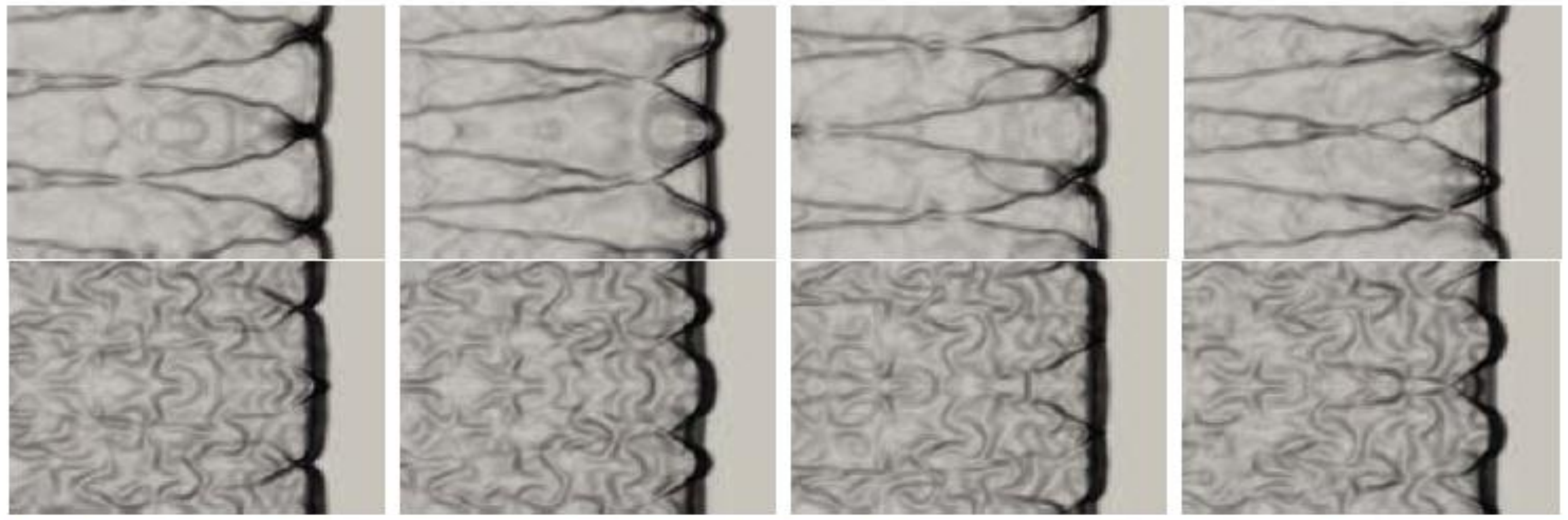

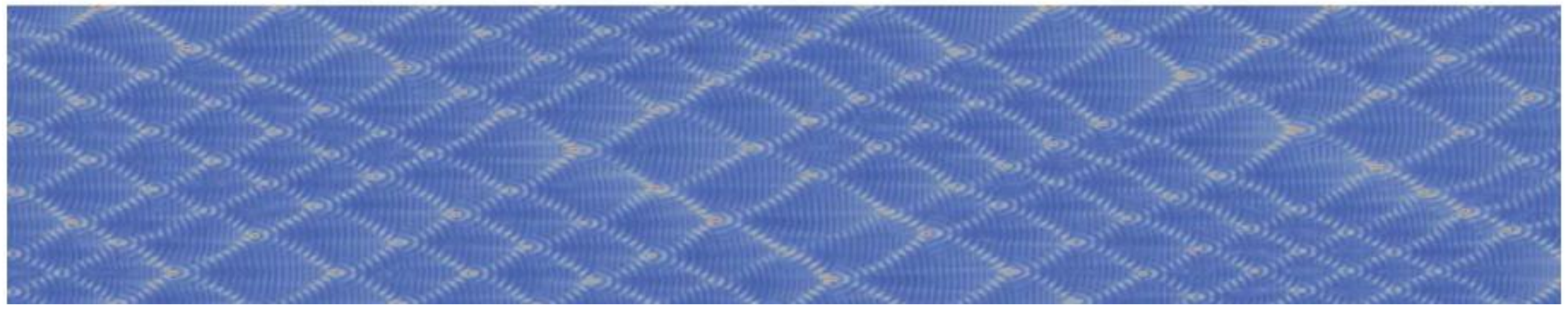

GPU parallelization

- Approaches
  - Cell-based (1 cell per thread) parallelization: EOS, time marching, chemistry, etc.
  - Face-based (1 face per thread) parallelization: Reconstruction, flux, etc.
- Optimization strategies
  - Coalesce memory access for optimal DRAM memory bandwidth
  - Utilize on-chip shared memory whenever possible
  - Reduce memory transfers between cpu and gpu
  - Adapt instruction level parallelism (ILP) with in GPU kernels by reducing block occupancy and utilizing more registers
- Message passing interface (MPI) for multiGPU computation
  - Domain decomposition
  - Boundary exchange

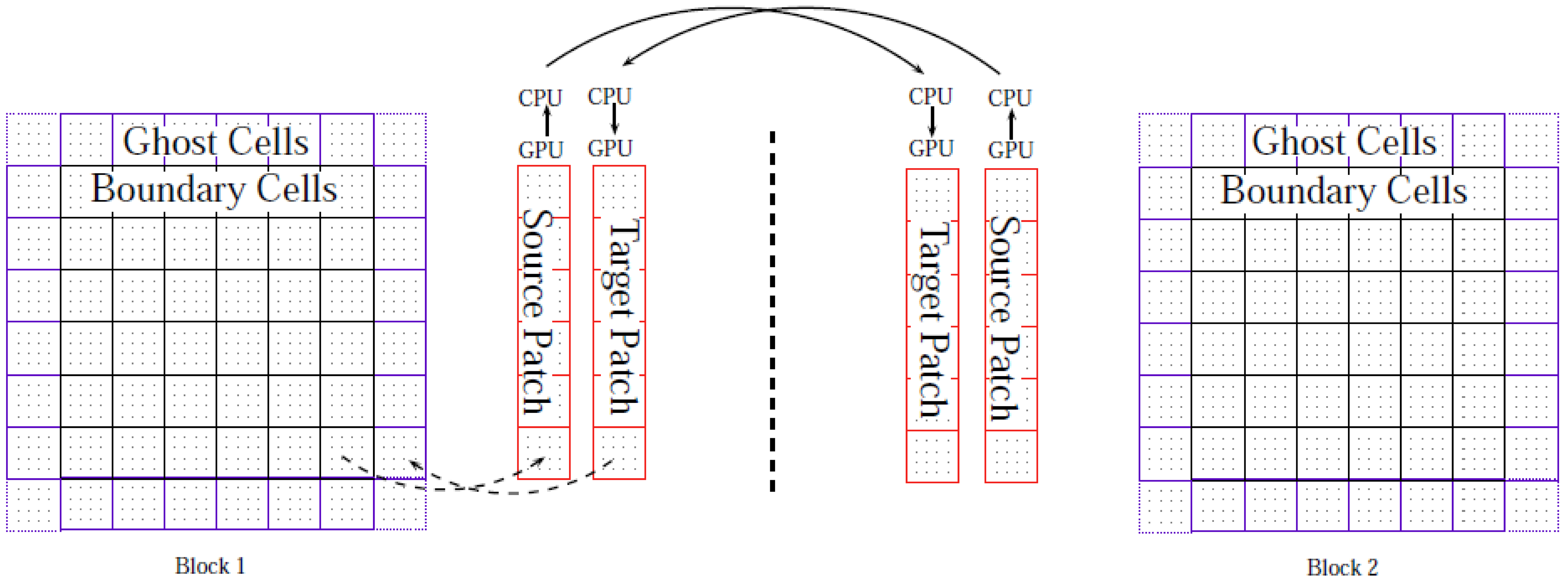

GPU vs. CPU

Comparison between NVIDIA Tesla M2070 and Intel Xeon X5650 (single core comparison)

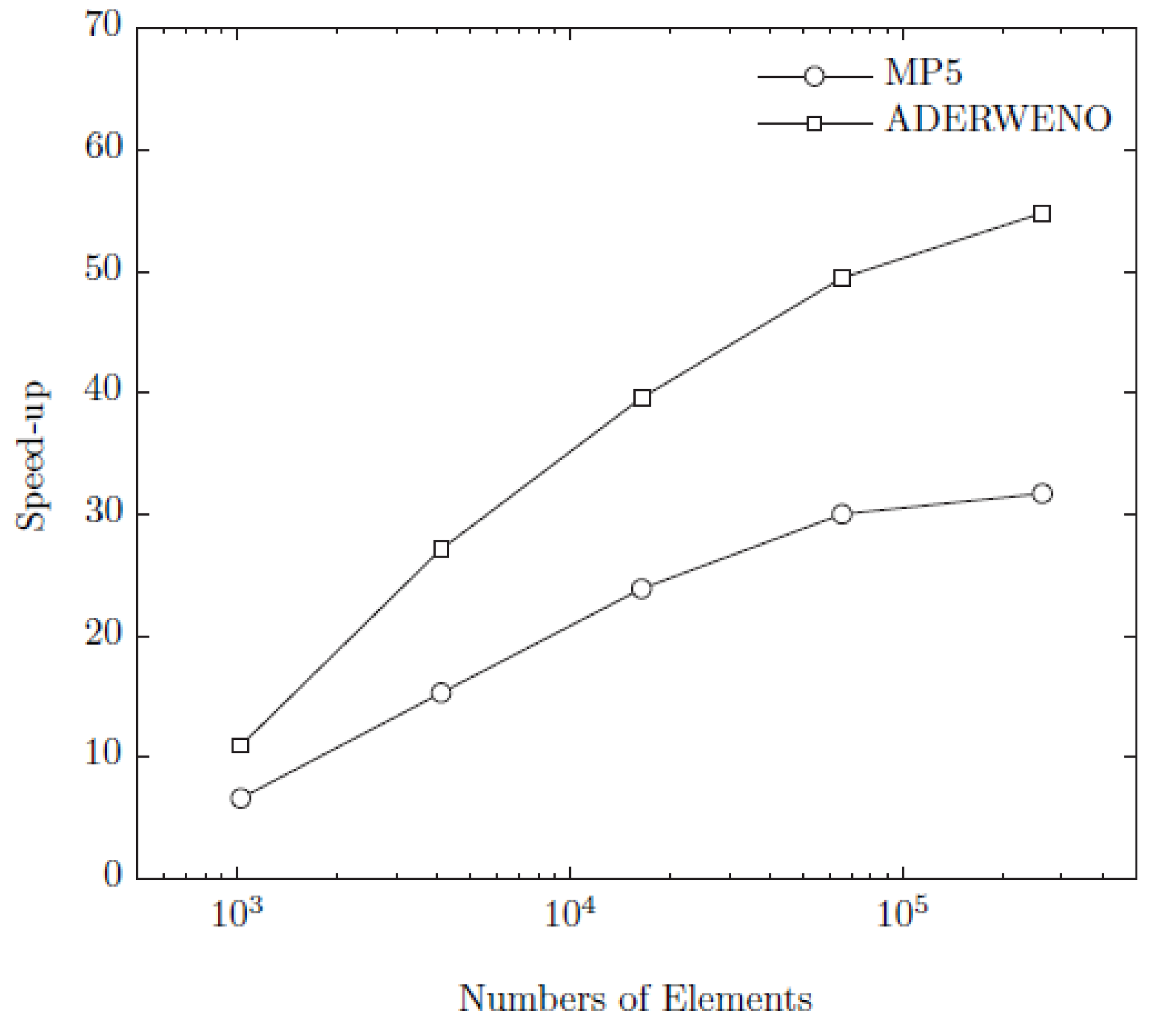

- Ideal Gas simulation (no chemical reaction)
  - 5th order accurate solutions (MP5 and ADERWENO)
  - Speedup factor up to 60

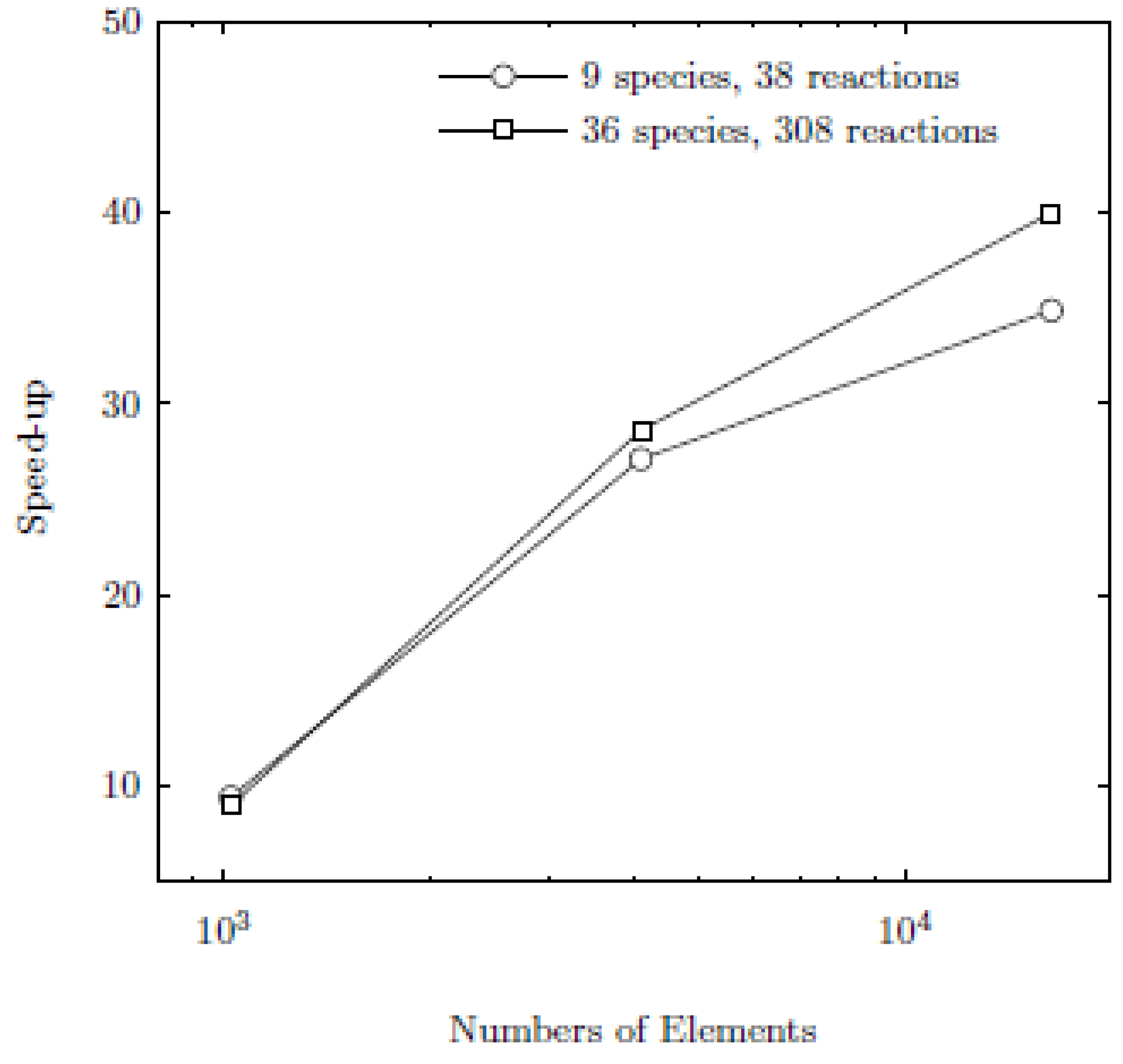

- Reacting flow simulation (detonation)
  - Comparison of two different mechanism: H_2-Air and CH_4-Air detonation
  - Speedup factor up to 40